Kobe University Repository : Kernel

PDF issue: 2026-11-26

Enhancing quantum imaging efficiency by BiBO crystal-based entangled light source

Yoshimura, Kanako

Yoneda, Naru

Matoba, Osamu

(Citation)
AIP Advances,16(6):065123

(Issue Date)
2026-06-01

(Resource Type)
journal article

(Version)
Version of Record

(Rights)
© 2026 Author(s).
All article content, except where otherwise noted, is licensed under a Creative Commons Attribution (CC BY) license

(URL)
https://hdl.handle.net/20.500.14094/0100504848

AIP Advances

RESEARCH ARTICLE | JUNE 12 2026

Enhancing quantum imaging efficiency by BiBO crystal-based entangled light source

Kanako Yoshimura ; Naru Yoneda ; Osamu Matoba

Check for updates

AIP Advances 16, 065123 (2026)
https://doi.org/10.1063/5.0314450

View Online
Export Citation

Connected Content

A companion article has been published: A better source of entangled photons for quantum imaging

Articles You May Be Interested In

Wind energy harvesting using jet-edge flow oscillations

AIP Advances (September 2018)

Analytical predictions of periodic oscillations in a piezoelectric energy harvester under combined aeroelastic and harmonic excitation

Chaos (April 2023)

Filler-depletion layer adjacent to interface impacts performance of thermal interface material

AIP Advances (January 2016)

25 June 2026 04:23:57

AIP Publishing

Special Topics Open for Submissions

Learn More

AIP Publishing

Enhancing quantum imaging efficiency by BiBO crystal-based entangled light source

Cite as: AIP Advances 16, 065123 (2026); doi: 10.1063/5.0314450
Submitted: 18 January 2026 • Accepted: 4 May 2026 •
Published Online: 12 June 2026

View Online Export Citation CrossMark

Kanako Yoshimura,[1,a] Naru Yoneda,[1,2,b] and Osamu Matoba[1,2]

AFFILIATIONS

[1] Department of System Science, Graduate School of System Informatics, Kobe University, Rokkodai 1-1, Nada, Kobe 657-8501, Japan
[2] Center of Optical Scattering Image Science, Kobe University, Rokkodai 1-1, Nada, Kobe 657-8501, Japan

[a] 248x093x@stu.kobe-u.ac.jp
[b] **Author to whom correspondence should be addressed:** yoneda.naru@port.kobe-u.ac.jp

ABSTRACT

Quantum imaging utilizing entangled photon pairs takes advantage of their strong quantum correlations to surpass the limitations of classical imaging techniques in terms of spatial resolution and signal-to-noise ratio. However, due to the low brightness of entangled photon sources, an enormous number of intensity images ($\sim 10^7$) is required for imaging in previous studies in order to acquire images with a sufficient signal-to-noise ratio, posing a challenge for practical implementation. A BiBO crystal, known for its large nonlinear optical coefficient, is considered a promising high-brightness entangled photon source. However, its performance has not been quantitatively evaluated in the context of quantum imaging systems, particularly regarding its impact on imaging performance. Here, we investigate the potential of a BiBO crystal as a light source for high-efficiency quantum imaging by performing parallel intensity correlation measurements and implementing quantum image distillation as an example in comparison with a commonly used BBO crystal. The results demonstrate that the use of the BiBO crystal enables more efficient quantum imaging compared to the conventional BBO crystal.

© 2026 Author(s). All article content, except where otherwise noted, is licensed under a Creative Commons Attribution (CC BY) license (https://creativecommons.org/licenses/by/4.0/). https://doi.org/10.1063/5.0314450

25 June 2026 04:23:57

Quantum imaging leverages the quantum properties of photons to surpass the fundamental limits of classical imaging.[1–4] Among existing non-classical light sources, methods utilizing the spatial correlations of entangled photon pairs are particularly attractive due to the ease of generating photon pairs via spontaneous parametric down-conversion (SPDC).[5,6] Furthermore, the advent of commercially available single-photon-sensitive cameras has facilitated the development of imaging systems based on such photon pairs.[7] These cameras can detect photon coincidences across multiple transverse spatial positions, which is crucial for imaging techniques that utilize entangled photon pairs. For example, EMCCD and SPAD cameras enable the detection of photon pairs across thousands of spatial modes and the evaluation of their entanglement state based on the second-order intensity correlation function.[8,9] As a result, imaging techniques based on photon pair intensity correlations have been increasingly explored, such as quantum holography that reconstructs holograms without interfering with object and reference beams,[10] super-resolution imaging,[11] and quantum image distillation as an imaging technique robust against noise.[12] Thanks to these recent technological advancements, constructing imaging systems based on photon pairs has become relatively easy to implement.

However, due to the low brightness of SPDC sources—that is, their low photon pair generation rate—acquiring sufficient data for correlation measurements requires an enormous amount of measurement time, often ranging from several tens of hours to over a day.[9,13] This constraint has confined quantum imaging applications primarily to laboratory environments and niche research fields, making them far from a viable replacement for classical imaging systems. Therefore, improving the efficiency and practicality of quantum imaging technologies is important.

Conventionally, SPDC processes for quantum imaging have predominantly employed a BBO crystal, a uniaxial nonlinear optical crystal, because of its relatively large second-order nonlinear optical coefficient. One approach to enhancing SPDC efficiency involves the use of thicker nonlinear optical crystals, which can increase

© Author(s) 2026

the occurrence of SPDC events. However, this approach is fundamentally limited because the crystal length is finite due to both practical and optical limitations. Moreover, increasing the crystal thickness improves the photon-pair generation efficiency, but it also increases the fluctuation in the photon-pair generation position, which leads to a degradation of spatial resolution when applied to quantum imaging. Another method is the use of high-intensity laser sources, although this carries the risk of crystal damage and inevitably involves high cost.

In this study, we demonstrate the use of a BiBO crystal for the generation of entangled photon pairs as a means to improve the efficiency of quantum imaging and demonstrate its effectiveness through imaging applications. The BiBO crystal is a biaxial nonlinear optical crystal that was introduced approximately two decades ago.[14] It possesses a nonlinear optical coefficient ~1.5–2.0 times larger than that of the commonly used uniaxial BBO crystal.[15,16] Due to its characteristics, the BiBO crystal is considered a promising candidate for realizing high-brightness SPDC sources.[17,18] Although quasi-phase matching (QPM) techniques, such as periodically poled crystals, can achieve higher SPDC efficiency than birefringent phase matching, the photon pairs they generate are typically emitted along collinear directions.[19] This may impose restrictions on the field of view when applied to quantum imaging. Furthermore, these techniques typically require precise temperature control and tend to be more expensive. For these reasons, we chose to employ the BiBO crystal with birefringent phase matching in this study.

While the high SPDC efficiency of BiBO crystals is known, their performance has not been quantitatively evaluated in the context of modern camera-based quantum imaging systems. This represents a critical gap in the field, as the practical impact of higher SPDC efficiency on the number of frames required for image reconstruction remains unclear.

Here, we address this gap by performing the first quantitative evaluation of the BiBO crystal in this application. We first evaluate the entangled states generated from two SPDC sources based on BBO and BiBO crystals, respectively, by employing parallel intensity correlation measurements.[20] Then, as an application to quantum imaging, we demonstrate quantum image distillation using both sources. By comparing the results obtained from the two sources, we show that the BiBO crystal-based SPDC source is beneficial for enhancing the efficiency of quantum imaging.

One of the key factors determining the efficiency of photon pair generation is the interaction between light and the nonlinear optical crystal during the SPDC process. Specifically, this interaction is described by the interaction Hamiltonian $\hat{H}_I(t)$ representing the coupling between the electric field of the pump light and the nonlinear polarization, as expressed by the following equation:[19]

$$\hat{H}_I(t) = \epsilon_0 \int_V \chi^{(2)} \hat{E}_p^{(+)}(\mathbf{r},t)\hat{E}_s^{(-)}(\mathbf{r},t)\hat{E}_i^{(-)}(\mathbf{r},t)d^3\mathbf{r} + \text{H.c.}, \quad (1)$$

where V is the volume of nonlinear optical crystal; ϵ_0 is the vacuum permittivity; $\chi^{(2)}$ is the second-order nonlinear susceptibility; $\hat{E}^{(+)}(t)$ and $\hat{E}^{(-)}(t)$ are the positive and negative frequency parts of the electric field operator, respectively; p, s, and i stand for pump, signal and idler, respectively, and H.c. stands for the Hermitian conjugate. The nonlinear optical coefficient of the crystal, often denoted as d, is derived from $\chi^{(2)}$ by the relation $d = \frac{\chi^{(2)}}{2}$. As shown in Eq. (1), the strength of this interaction depends on the nonlinear optical coefficient of the crystal. A larger nonlinear optical coefficient leads to a higher probability of photon pair generation. Since the probability of photon pair generation rate in SPDC is theoretically proportional to the square of the nonlinear optical coefficient,[21] using a crystal with a larger nonlinear optical coefficient enables the realization of a high-brightness photon source.

By using an EMCCD camera, it is possible to perform large-scale and parallel correlation measurements of photon pairs.[7,20] This intensity correlation measurement is crucial not only for evaluating the coincidence of entangled photon pairs but also as a fundamental technique for quantum imaging methods that utilize spatial correlations.

Values of intensity correlation between a pixel $\mathbf{k}_1$ and $\mathbf{k}_2$ are calculated by subtracting the product of the intensity values measured in the same frame from the product of the intensity values measured in successive frames and averaging over all the frames,

$$\Gamma(\mathbf{k}_1,\mathbf{k}_2) = \frac{1}{N}\sum_{n=1}^{N} I_n(\mathbf{k}_1)I_n(\mathbf{k}_2) - \frac{1}{N-1}\sum_{n=1}^{N-1} I_n(\mathbf{k}_1)I_{n+1}(\mathbf{k}_2), \quad (2)$$

where I_n denotes the intensity image obtained in the nth frame of the camera. Because the exposure and readout time of the EMCCD camera are significantly longer than the correlation times of photon pairs, the first term includes some accidental coincidence. Therefore, subtracting the second term allows us to eliminate accidental

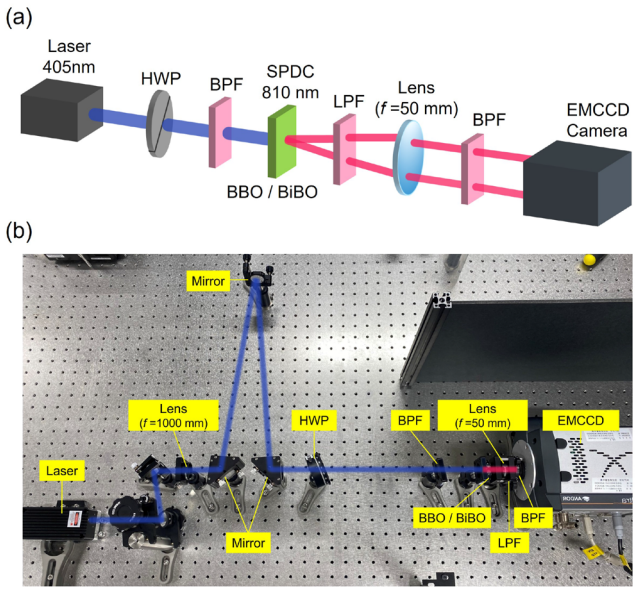

FIG. 1. (a) Experimental setup scheme for measuring the momentum correlation. A pump laser (λ_p = 405 nm) is guided through a Half-Wave Plate (HWP) for polarization control. The generated photon pairs (centered wavelength at 810 nm) are detected by an EMCCD camera via a lens (f = 50 mm). To ensure that only photons of the desired wavelength are used, a band-pass filter (BPF) and a long-pass filter (LPF) are placed. (b) Image of a laboratory setup.

25 June 2026 04:23:57

© Author(s) 2026

coincidence counts and obtain the pure coincidence probability. A detailed explanation of this expression can be found in Ref. 7.

Figure 1(a) shows the schematic and a photograph of the experimental setup to measure the momentum correlation of the photon pairs generated using either a BBO or BiBO crystal. This configuration is designed to generate entangled photon pairs at a wavelength of 810 nm. To ensure that only photons of the desired wavelength are used, a band-pass filter (405 nm, FWHM 10 nm) is placed before the crystal, while a long-pass filter (transmitting wavelengths above 550 nm) and a band-pass filter (800 nm, FWHM 40 nm) are inserted after the crystal. As shown in Fig. 1(b), the laser beam is weakly focused onto the crystal using a lens with a focal length of 1000 mm to enhance the efficiency of SPDC. Details of an experimental condition are provided in the supplementary material.

Figure 2 shows the comparison of intensity correlation measurements between the use of BBO and BiBO crystals. The integrated intensity image obtained using the BBO crystal is shown in Fig. 2(a), and the correlation measurement results Γ are shown in Fig. 2(c). Similarly, the integrated intensity image obtained using the BiBO crystal is shown in Fig. 2(b), and the correlation measurement results Γ are shown in Fig. 2(d). Each correlation measurement is the result of photons detected at pixel **k**. For both crystals, the pump laser intensity was kept the same, and the intensity correlation measurements were performed using a total of $N = 10^6$ intensity images with an exposure time of 3 ms. This exposure time was chosen following Refs. 10 and 22. Here, since the effective nonlinear optical coefficient depends on the phase-matching condition, the difference in the nonlinear optical coefficients between BBO and BiBO can be evaluated by precisely adjusting the crystal angle.

In the case of the BBO crystal [Fig. 2(c)], no correlation peak is observed, whereas in the case of the BiBO crystal [Fig. 2(d)], a correlation peak is served around pixel $-\mathbf{k}$. This correlation peak indicates that when one photon is detected at pixel **k**, its twin photon is localized around pixel $-\mathbf{k}$, reflecting the momentum correlation between photons in the SPDC process. The difference in the size of the ring pattern for each crystal is due to the rotation of the optical axis in the direction of the pump light travel axis during the crystal replacement, which changed the combination of signals and idlers that satisfy the phase matching condition.

Figure 3(a) shows a graph of the variation in the contrast-to-noise ratio (CNR) with the number of intensity images used in the intensity correlation measurement. The experimental data were fitted with a $\sqrt{N}$ dependence, as described in Refs. 23 and 24. The CNR was calculated following the method described in Ref. 11, and detailed calculation procedures can be found in the supplementary material. When using a million frames, the correlation map obtained with a BiBO crystal achieved a CNR ~5.6 times higher than that obtained with a BBO crystal. This difference in the results may also

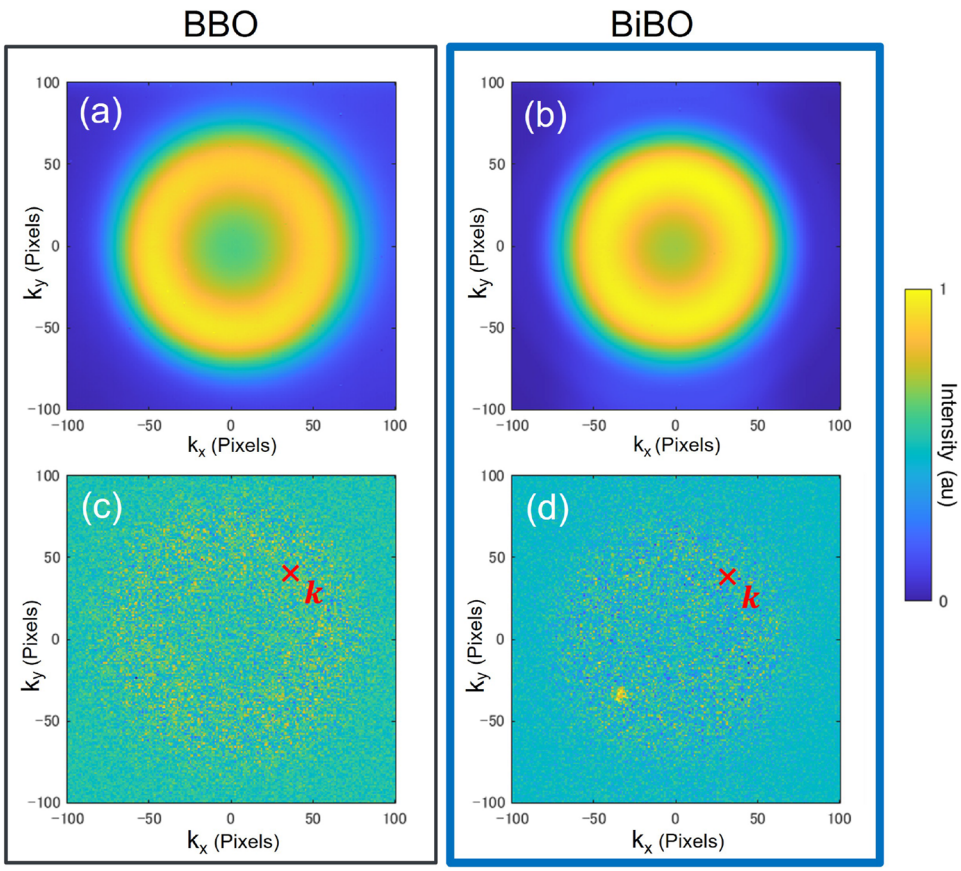

FIG. 2. Results of intensity correlation measurement. The integrated intensity image obtained using (a) the BBO crystal and (b) the BiBO crystal. The intensity correlation measurement results for the pixel indicated by **k** obtained using (c) the BBO crystal and (d) the BiBO crystal. Each intensity correlation measurement was performed using $N = 10^6$ intensity images with an exposure time of 3 ms.

25 June 2026 04:23:57

© Author(s) 2026

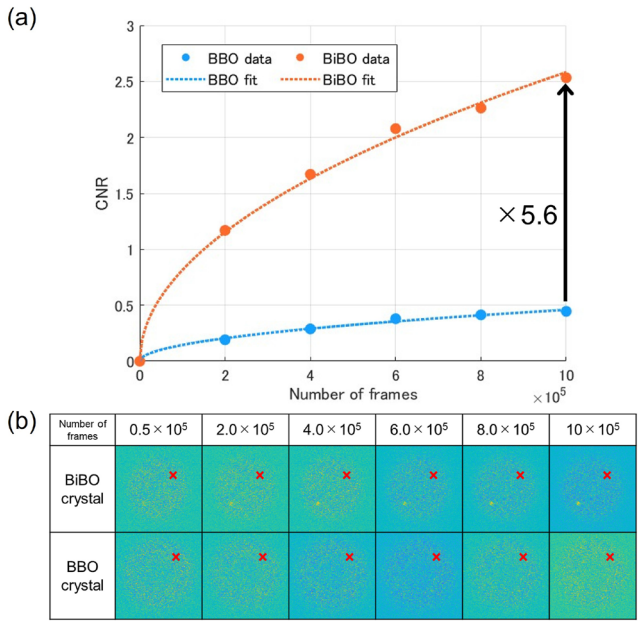

FIG. 3. Variation of (a) CNRs and (b) intensity correlation maps with increasing number of intensity images for BiBO and BBO crystals. The experimental data are shown as dots, and fits are shown as dashed lines.

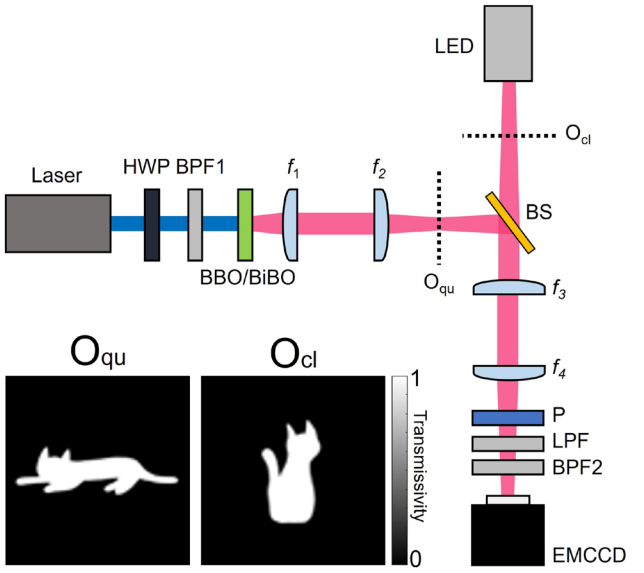

FIG. 4. Experimental setup. A CW laser (λ_p = 405 nm) pumps the nonlinear optical crystal to generate spatially entangled pairs. A band-pass filter1 (BPF1, center wavelength 405 nm, FWHM 10 nm) is placed before the crystal. Lenses f_1 = 50 mm and f_2 = 200 mm image the crystal surface onto an object O_{qu} (a dead cat). Simultaneously, an object O_{cl} (alive cat) is illuminated by an 800 nm-LED, and both objects are imaged onto the image sensor through a beam splitter (BS; 90% transmission) and lenses f_3 = 100 mm and f_4 = 100 mm. A polarizer (P), a long-pass filter (LPF, transmitting wavelengths above 550 nm), and a band-pass filter (BPF2, center wavelength 800 nm, FWHM 40 nm) placed in front of the camera were used to select near-degenerate photons. Each object consists of a glass substrate coated with evaporated chromium.

reflect a difference in the heralding efficiency. Figure 3(b) shows the correlation maps corresponding to each number of frames used. When using the BiBO crystal, the correlation peak becomes visible more rapidly, demonstrating the higher efficiency of the correlation measurement.

Next, as an application of imaging techniques, we performed quantum image distillation.[12] Quantum image distillation is an experimental technique that obtains quantum images from camera measurements containing both quantum and classical images by exploiting the spatial correlations inherent in entangled photon pairs. Figure 4 shows the optical setup used for quantum image distillation. Entangled photon pairs at a wavelength of 810 nm are generated from 405 nm pump photons via SPDC using either a BBO or BiBO crystal. The SPDC photons emitted from the source constructed in previous experiments are imaged onto the object O_{qu} (a dead cat) through lenses f_1 and f_2. Simultaneously, classical object O_{cl} (an alive cat) is illuminated by an 800 nm-LED and imaged onto the same image sensor via a beam splitter (BS) so that the images of both objects are superimposed on the camera. Because both object images have the same wavelength and polarization components, they cannot be distinguished from the raw intensity image obtained by the camera. However, LED photons are uncorrelated, whereas SPDC photons exhibit spatial correlations at the point of generation. Therefore, by exploiting these correlations and integrating the intensity correlation function [Eq. (2)] over all pixels, only contributions from entangled photon pairs remain. Contributions vanish, and only correlated SPDC terms remain. As the correlated pairs uniformly illuminate the object, this integral becomes proportional to the shape of the quantum object O_{qu}, enabling selective reconstruction using quantum illumination.

Using the optical system shown in Fig. 4, a comparative study was conducted employing either a BBO or a BiBO crystal. For each crystal, a total of 3.5×10^6 intensity images were acquired and used for quantum image distillation. The pump beam intensity was kept at 22 mW for both cases. The integrated intensity image obtained using the BBO crystal is shown in Fig. 5(a), and the reconstructed image via quantum image distillation is shown in Fig. 5(c). Similarly, Fig. 5(b) shows the integrated intensity image obtained using the BiBO crystal, and Fig. 5(d) shows the corresponding reconstructed image. When using the BBO crystal, the two cat images (quantum and classical) could not be separated. In contrast, with the BiBO crystal, only the object O_{qu} illuminated by the SPDC source (that is, the dead cat) is visible, successfully separating the two images. Although the reconstructed image does not have a uniform distribution, this is due to the non-uniformity of illumination. Variations in correlation values caused by differences in photon counts are expected to be averaged out when a sufficient number of frames is used, resulting in a reconstructed image that closely reflects the original spatial distribution of the entangled photons.

Figure 6(a) shows the CNR as a function of the number of image frames used. Detailed calculation procedures can be found in the supplementary material. When 3.5×10^6 frames were used, the CNR was 0.76 for the BBO crystal and 4.36 for the BiBO crystal. In other words, using the BiBO crystal resulted in a CNR

25 June 2026 04:23:57

© Author(s) 2026

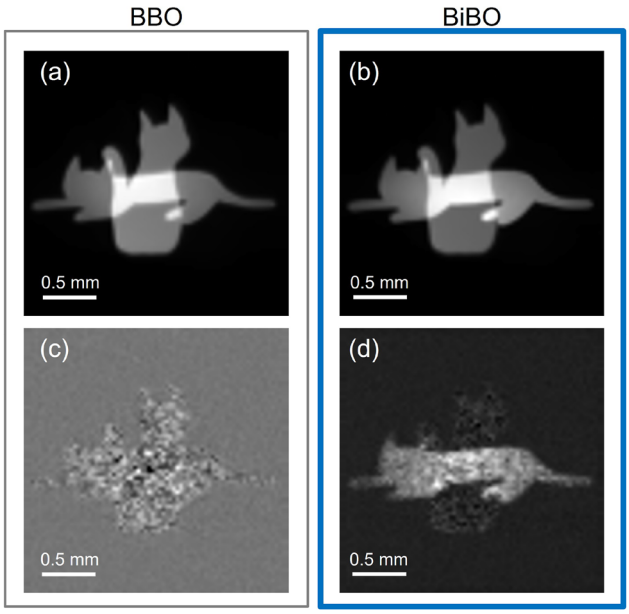

FIG. 5. Results of quantum image distillation. The integrated intensity image obtained using (a) the BBO crystal and (b) the BiBO crystal. Reconstructed image obtained using (c) the BBO crystal and (d) the BiBO crystal. Each image was reconstructed from $N = 3.5 \times 10^6$ intensity images with an exposure time of 3 ms.

~5.7 times higher than that of the BBO crystal, demonstrating a significant improvement in the efficiency of quantum image distillation. Figure 6(b) shows the reconstructed images corresponding to each number of frames used. When using the BiBO crystal, the

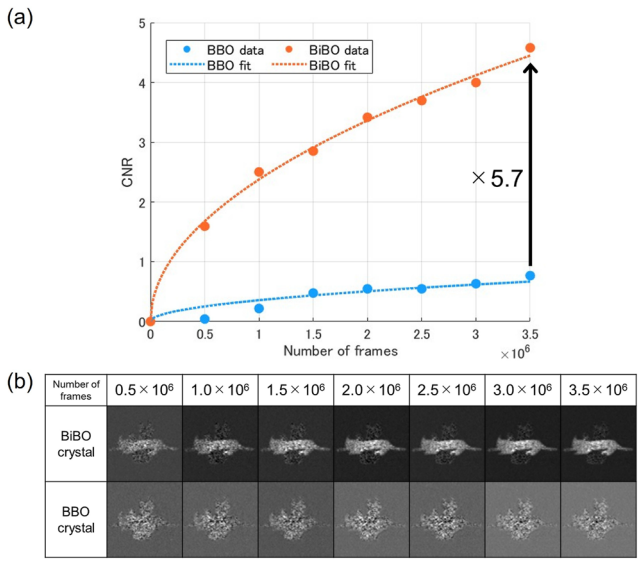

FIG. 6. Variation of (a) CNRs and (b) reconstructed images with increasing number of intensity images for the BiBO and BBO crystal. The experimental data are shown as dots, and fits are shown as dashed lines.

two cat images become clearly separated even at 10^6 frames, indicating a rapid acquisition capability. In contrast, the BBO crystal failed to achieve a comparable level of clear image separation and noise suppression even after acquiring the maximum number of 3.5×10^6 frames. This result shows that the BiBO crystal-based light source not only provides quantitatively superior performance but also achieves a qualitatively successful image reconstruction within a measurement duration where the BBO crystal-based light source falls short. Thus, quantum image distillation is achieved significantly more efficiently with the BiBO crystal-based light source.

It is important to note that the BBO crystal results presented here reflect its performance under low-flux experimental conditions, which were deliberately chosen to ensure a fair comparison with the BiBO crystal within the same short measurement time. The previous study employing the BBO crystal achieved reconstruction of the image on the frame order of 10^6[12] but used a longer exposure time (6 ms) and a higher pump power (~50 mW) than those used in this work (3 ms and 22 mW, respectively). The successful performance of the BiBO crystal under such limited photon flux conditions clearly underscores its superior efficiency.

We demonstrated that the adoption of a BiBO crystal for the generation of entangled photon pairs leads to enhanced efficiency in quantum imaging. To evaluate its performance, we conducted parallel intensity correlation measurements and applied quantum image distillation as an example. The experimental results confirm that the BiBO crystal-based entangled light source exhibits superior imaging efficiency compared to the commonly used BBO crystal-based entangled light source. This work presents the first quantitative evaluation of the well-known high efficiency of a BiBO crystal in the context of recently developed camera-based quantum imaging and shows its implications for practical application. The efficiency of quantum imaging can be pursued along two complementary technical routes: increasing the number of detected signal photons through high-brightness photon sources and reducing accidental coincidences by employing high-speed detectors. In particular, the use of high-brightness sources raises concerns about an increased rate of accidental coincidences. Recent advances in single-photon sensitive time-stamping cameras, such as SPAD cameras and intensified time-stamping cameras (e.g., Tpx3Cam), enable coincidence measurements with nanosecond temporal resolution. These developments allow accidental coincidences to be effectively suppressed, thus improving the quality of reconstructed images.[9,25–27] Therefore, combining a BiBO-based SPDC source with a high-speed detector is expected to maximize true coincidences while minimizing noise, providing a concrete pathway toward efficient and scalable quantum imaging. The use of a BiBO crystal is expected to be beneficial for other quantum imaging techniques, such as quantum ghost imaging.

The supplementary material includes the following sections: details of the experimental setup, measurement of photon counting rate, contrast-to-noise ratio estimation, momentum correlation measurements, measuring EPR entanglement, quantifying entanglement in high-dimensional quantum image distillation, and quantum image distillation with another object.

The authors thank Professor Susumu Fukatsu at the University of Tokyo for providing information on BiBO crystals. The

25 June 2026 04:23:57

© Author(s) 2026

authors thank Mr. Jin Ozawa at the Tokyo University of the Arts for designing the cats shown in Fig. 4.

This research is supported by the JSPS KAKENHI (Grant Nos. 20H05886, 23K17749) and the JST, PRESTO (Grant No. JPMJPR25FA).

AUTHOR DECLARATIONS

Conflict of Interest

The authors have no conflicts to disclose.

Author Contributions

Kanako Yoshimura: Conceptualization (equal); Data curation (equal); Investigation (lead); Software (lead); Validation (lead); Writing – original draft (lead). **Naru Yoneda**: Conceptualization (equal); Funding acquisition (equal); Project administration (lead); Writing – review & editing (equal). **Osamu Matoba**: Conceptualization (equal); Funding acquisition (lead).

DATA AVAILABILITY

The data that support the findings of this study are available from the corresponding author upon reasonable request.

REFERENCES

[1]P.-A. Moreau, E. Toninelli, T. Gregory, and M. J. Padgett, "Imaging with quantum states of light," Nat. Rev. Phys. **1**, 367 (2019).
[2]N. Treps, U. Andersen, B. Buchler, P. K. Lam, A. Maître, H.-A. Bachor, and C. Fabre, "Surpassing the standard quantum limit for optical imaging using nonclassical multimode light," Phys. Rev. Lett. **88**, 203601 (2002).
[3]I. P. Degiovanni, M. Bondani, E. Puddu, A. Andreoni, and M. G. A. Paris, "Intensity correlations, entanglement properties, and ghost imaging in multimode thermal-seeded parametric down-conversion: Theory," Phys. Rev. A **76**, 062309 (2007).
[4]H. Defienne, P. Cameron, B. Ndagano, A. Lyons, M. Reichert, J. Zhao, A. R. Harvey, E. Charbon, J. W. Fleischer, and D. Faccio, "Pixel super-resolution with spatially entangled photons," Nat. Commun. **13**, 3566 (2022).
[5]S. P. Walborn, C. H. Monken, S. Pádua, and P. H. Souto Ribeiro, "Spatial correlations in parametric down-conversion," Phys. Rep. **495**, 87 (2010).
[6]J. Schneeloch and J. C. Howell, "Introduction to the transverse spatial correlations in spontaneous parametric down-conversion through the biphoton birth zone," J. Opt. **18**, 053501 (2016).
[7]H. Defienne, M. Reichert, and J. W. Fleischer, "General model of photon-pair detection with an image sensor," Phys. Rev. Lett. **120**, 203604 (2018).
[8]M. P. Edgar, D. S. Tasca, F. Izdebski, R. E. Warburton, J. Leach, M. Agnew, G. S. Buller, R. W. Boyd, and M. J. Padgett, "Imaging high-dimensional spatial entanglement with a camera," Nat. Commun. **3**, 984 (2012).
[9]B. Ndagano, H. Defienne, A. Lyons, I. Starshynov, F. Villa, S. Tisa, and D. Faccio, "Imaging and certifying high-dimensional entanglement with a single-photon avalanche diode camera," npj Quantum Inf. **6**, 94 (2020).
[10]H. Defienne, B. Ndagano, A. Lyons, and D. Faccio, "Polarization entanglement-enabled quantum holography," Nat. Phys. **17**, 591 (2021).
[11]Z. He, Y. Zhang, X. Tong, L. Li, and L. V. Wang, "Quantum microscopy of cells at the Heisenberg limit," Nat. Commun. **14**, 2441 (2023).
[12]H. Defienne, M. Reichert, J. W. Fleischer, and D. Faccio, "Quantum image distillation," Sci. Adv. **5**, eaax0307 (2019).
[13]P. Cameron, B. Courme, D. Faccio, and H. Defienne, "Shaping the spatial correlations of entangled photon pairs," J. Phys.: Photonics **6**, 033001 (2024).
[14]P. Becker, J. Liebertz, and L. Bohatý, "Top-seeded growth of bismuth triborate, BiB_3O_6," J. Cryst. Growth **203**, 149 (1999).
[15]H. Hellwig, J. Liebertz, and L. Bohatý, "Exceptional large nonlinear optical coefficients in the monoclinic bismuth borate BiB_3O_6 (*BIBO*)," Solid State Commun. **109**, 249 (1998).
[16]M. Ghotbi and M. Ebrahim-Zadeh, "Optical second harmonic generation properties of BiB_3O_6," Opt. Express **12**, 6002 (2004).
[17]R. Rangarajan, M. Goggin, and P. Kwiat, "Optimizing type-I polarization-entangled photons," Opt. Express **17**, 18920 (2009).
[18]H. E. Guilbert, Y.-P. Wong, and D. J. Gauthier, "Observation of elliptical rings in type-I spontaneous parametric downconversion," J. Opt. Soc. Am. B **32**, 2096 (2015).
[19]S. Karan, S. Aarav, H. Bharadhwaj, L. Taneja, A. De, G. Kulkarni, N. Meher, and A. K. Jha, "Phase matching in β-barium borate crystals for spontaneous parametric down-conversion," J. Opt. **22**, 083501 (2020).
[20]M. Reichert, H. Defienne, and J. W. Fleischer, "Massively parallel coincidence counting of high-dimensional entangled states," Sci. Rep. **8**, 7925 (2018).
[21]J. Schneeloch, S. H. Knarr, D. F. Bogorin, M. L. Levangie, C. C. Tison, R. Frank, G. A. Howland, M. L. Fanto, and P. M. Alsing, "Introduction to the absolute brightness and number statistics in spontaneous parametric down-conversion," J. Opt. **21**, 043501 (2019).
[22]C. Vernière and H. Defienne, "Hiding images in quantum correlations," Phys. Rev. Lett. **133**, 093601 (2024).
[23]H. Defienne, M. Reichert, and J. W. Fleischer, "Adaptive quantum optics with spatially entangled photon pairs," Phys. Rev. Lett. **121**, 233601 (2018).
[24]M. Reichert, H. Defienne, and J. W. Fleischer, "Optimizing the signal-to-noise ratio of biphoton distribution measurements," Phys. Rev. A **98**, 013841 (2018).
[25]B. Courme, C. Vernière, P. Svihra, S. Gigan, A. Nomerotski, and H. Defienne, "Quantifying high-dimensional spatial entanglement with a single-photon-sensitive time-stamping camera," Opt. Lett. **48**, 3439 (2023).
[26]R. Guitter, B. Courme, C. Vernière, P. Svihra, A. Nomerotski, and H. Defienne, "Accidental coincidences in camera-based high-dimensional entanglement certification," Opt. Lett. **50**, 7532 (2025).
[27]A. Mavian, Y. Xu, C. Li, and R. W. Boyd, "Fast quantum ghost imaging with a single-photon-sensitive time-stamping camera," Opt. Lett. **50**, 594 (2025).

25 June 2026 04:23:57

© Author(s) 2026